Pakistan Veterinary Journal

ISSN: 0253-8318 (PRINT), 2074-7764 (ONLINE)
DOI: 10.29261/pakvetj/2025.253

RESEARCH ARTICLE

Rnai-Mediated Silencing of Superoxide Dismutase in *Toxocara Canis* Affects the Development and Survival of Eggs and Larvae

Tian-Le Wu [1], Bing-Nan Wang [2], Bin-Yu Li [1], Zi-Ying Hu [1], Yi-Ning You [1], Yong-Li Luo [3], Shi-Cheng Bi [1] and Rong-Qiong Zhou [1, *]

[1] College of Veterinary Medicine, Southwest University, Chongqing 402460, China; [2] Chongqing College of Chinese Medicine, Chongqing 402760, China; [3] College of Animal Science and Technology, Chongqing Three Gorges Vocational College, Chongqing 404155, China
*Corresponding author: rongqiongzhou@126.com

ARTICLE HISTORY (25-474)

Received: May 06, 2025
Revised: August 21, 2025
Accepted: August 22, 2025
Published online: September 29, 2025

Key words:
Biological function
Infection
RNAi
Superoxide dismutase
Toxocara canis

ABSTRACT

Toxocara canis, a zoonotic parasitic nematode and one of the primary pathogens of human toxocariasis, poses a serious threat to public health and biosafety. As a pivotal component of the antioxidant system, superoxide dismutase (*sod*) promotes parasite resistance to oxidative damage and sustains their survival. This study characterized *Tc-sod* and investigated its expression patterns and tissue localization. The RNA interference (RNAi) was employed to examine the function of *Tc-sod* in the growth, development, and pathogenicity of *T. canis*. The results indicated that *Tc-sod* is expressed in female, male, and L3 larvae, and the immunofluorescence shows that it is mainly localized in the ovary, uterus, and body wall of *T. canis*, suggesting that *Tc-sod* is involved in the growth, development, and reproductive processes of *T. canis*. Compared with the PBS group, the *Tc-sod*-siRNA-61 significantly reduced the mRNA transcription and protein expression of *Tc-sod*, suggesting that siRNA-61 mediated specific silencing of the *Tc-sod* gene. It further affected the hatching rate of eggs, leading to phenotypic changes, including embryonic development disorders and larvae deformation. The larvae burden rate of infected mice in the *Tc-sod*-siRNA-61 group was 33.4%, and the motility of larvae was weakened. Mice in the *Tc-sod*-siRNA-61 group showed reduced haemorrhagic lesions and inflammatory infiltration in the liver, lungs, and brain tissues. These results demonstrate that *Tc-sod* is crucial in the development and survival of *T. canis*. It could also be a target candidate for the anti-*T. canis* vaccine and drugs.

To Cite This Article: Wu TL, Wang BN, Li BY, Hu ZY, You YN, Luo YL, Bi SC and Zhou RQ 2025. Rnai-Mediated silencing of superoxide dismutase in *Toxocara canis* affects the development and survival of eggs and larvae. Pak Vet J. http://dx.doi.org/10.29261/pakvetj/2025.253

INTRODUCTION

Toxocara canis is a significant and highly prevalent intestinal parasite, commonly found in tropical and subtropical regions of the world (Roldán *et al*., 2010; Chen *et al*., 2018; Ma *et al*., 2018; Rostami *et al*., 2020). Transmission occurs via ingestion of embryonated eggs from contaminated environmental sources (water, soil, fruits, and vegetables) or infective larvae in undercooked meat/viscera of paratenic hosts (Bowman, 2020; Healy *et al*., 2022, 2023; Yang *et al*., 2024). In definitive hosts (e.g., dogs and wolves), the infective larvae complete their life cycle in the intestine, developing into adults. In contrast, when human and other paratenic hosts (e.g., rabbits, rats, and chickens) ingest eggs, the infective larvae hatch in the small intestine and enter the circulatory system through the intestinal wall (Lopez-Alamillo *et al*., 2025). The L3 larvae migrate to tissues and organs, including muscles, nerves, and viscera, causing mechanical and immunopathological damage (Strube *et al*., 2013; Fava *et al*., 2020; Auer *et al*., 2020). Infection in humans typically leads to various clinical presentations, including asthma, muscle aches, skin allergies, heart disease, and neurological disorders (Ma *et al*., 2018; Rostami *et al*., 2019; Taghipour *et al*., 2021). It is estimated that about 1.4 billion people worldwide are infected with or exposed to *Toxocara* spp, posing a threat to human health and global public security (Rostami *et al*., 2019; Ma *et al*., 2020).

Previous draft genome, transcriptome, small non-coding RNAs, and secretome studies on *T. canis* explored invaluable data involved in the growth, reproduction, and host-parasite interactions of *T. canis* and improved the

In Press

understanding of the genetic constitution (Zhu *et al*., 2015; Ma *et al*., 2016; Zhou *et al*., 2017; da Silva *et al*., 2018; Zheng *et al*., 2020). Although numerous antigens are expressed during the *T. canis* developmental life cycle, including *Tc*-PEBP, *Tc*-MUC-1, and *Tc*-CTL-4, their functional verification requires further research (Li *et al*., 2021; Zhou *et al*., 2022; Abou-El-Naga *et al*., 2023; Wu *et al*., 2024). The multiple roles of parasites in exerting immune escape strategies and causing pathogenic damage are mediated by parasite-secreted effector molecules, which play a role both in the induction of the host immune response and host pathology, and in parasite metabolism and survival (Crowe *et al*., 2017; Da Silva *et al*., 2018; Abou-El-Naga *et al*., 2023).

Superoxide dismutase uses different metal cofactors to convert superoxide anions($O_2^{\bullet-}$) into molecular oxygen and hydrogen peroxide (H_2O_2), playing a critical role in antioxidant defense (Miller *et al*., 2012; Broxton and Culotta., 2016; Borgstahl and Oberley., 2018). Survival of *Leishmania amazonensis* and *L. braziliensis* in the host depends on this process (Khouri *et al*., 2009). Several isoforms of SOD have been described in helminths and their mammalian hosts based on their localisation and metal cofactors, including Cu/Zn-SOD (Cytosolic) (Extracellular), and Fe/Mn-SOD (Mitochondrial), which have converged and evolved from different ancestral genes (Cardoso *et al*., 2004). Previous investigations have revealed that a series of biological processes, such as anti-oxidative stress and maintaining homeostasis of the internal environment, mediated by SOD, are integral to the survival strategies of the parasite. For example, *microfilaria* and adult worms of *Onchocerca volvulus* produce SOD during migration and sojourning within host tissues, decreasing ROS release and enhancing survival of the parasite (Moustafa *et al*., 2022). In addition, the SOD also acts as an immune effector molecule, activating the host's protective immune response and preventing parasite invasion and adhesion (*Schistosoma mansoni, Taenia solium*, *Fasciola hepatica*, and *Toxoplasma gondii*) (Shalaby *et al*., 2003; Vaca-Paniagua *et al*., 2008; Lalrinkima *et al*., 2015; Jaikua *et al*., 2016; Liu *et al*., 2017). Despite these insights, the molecular features and biological roles of SOD in *T. canis* remain uncharacterized.

This study aims to characterize the function of *Tc-sod* through enzyme activity identification, expression pattern analysis, and RNAi; to determine the potential role of *Tc-sod* in the development, survival, and pathogenic processes of *T. canis*. These findings may contribute fundamental information for a deeper understanding of the functional significance of *Tc-sod* in *T. canis*.

MATERIALS AND METHODS

Parasites and experimental animals: Puppies testing positive for *T. canis* eggs in the faeces underwent clinical examination at the Animal Hospital of the College of Veterinary Medicine, Southwest University, China. The *T. canis* were collected from the faeces of infected dogs, post-anthelmintic treatment with Albendazole 25mg/kg BW and subjected to morphological and molecular biology identification. The infective eggs were obtained using previous methods with slight modifications (Zheng *et al*., 2021; Raulf *et al*., 2021). Briefly, eggs were harvested from the first third of the female *T. canis* uterus, and these fertilized eggs were placed in a culture dish (containing defatted cotton and filter paper and sterilized under high pressure), incubating at 28°C for 3-4 weeks in a constant temperature incubator. The eggs (containing infective L3 larvae) were washed repeatedly with sterile distilled water to remove impurities before use. Then, the larvae were hatched and collected through a funnel device (Bellman method) (Fan *et al*., 2003).

The male Kunming mice (18-22g, aged 6 weeks) and rabbits (about 2kg) were purchased from the Experimental Animal Center of Southwest Medical University. All animals were housed in suitable cages and provided with food and clean water.

Bioinformatics analysis of *Tc-sod:* The full-length sequence of *Tc-sod* (Cu/Zn-SOD) was retrieved from the NCBI (GenBank accession no: AAB00227.1). The molecular characteristics of *Tc-sod* were determined using multiple bioanalytical software and servers. The possible signal peptides and transmembrane regions were predicted by SignalP Server 6.0 (https://services.healthtech.dtu.dk/services/SignalP-6.0/) and TMHMM (https://services.healthtech.dtu.dk/services/TMHMM-2.0/), respectively. The protein structure model and functional prediction of *Tc*-SOD were constructed by the Iterative Threading ASSEmbly Refinement (I-TASSER) (https://zhanggroup.org/I-TASSER/) (Yang *et al*., 2015, Zhang *et al*., 2017, Zheng *et al*., 2021).

Expression of *Tc*-SOD recombinant protein and anti-*Tc*-SOD polyclonal antibody: Total RNA was isolated from *T. canis* using Trizol (Invitrogen, USA) and then reverse transcribed into cDNA (TaKaRa, China). The *Tc-sod* encoding sequence was amplified by PCR using forward primer 5'-CGCGGATCCATGCAAAGACCAAATTCA-3' (*Bam H*I) and reverse primer 5'-CCGCTCGAGTTACGGTGCGCCTGAGCT-3' (*Xho*I). The PCR product was purified and cloned into the expression vector pET-32a (Tsingke Biology, Beijing, China) at the *Bam H*I and *Xho*I restriction endonuclease sites. After verification of the sequence, the recombinant plasmid was transformed into *Escherichia coli* BL21 (DE3). The recombinant SOD was expressed by 0.4mM IPTG induction (Sangon, Shanghai, China) at 37°C for 8h and purified with a Ni-NTA affinity chromatography. The concentration of the recombinant protein was estimated by BCA kit (Beyotime, Shanghai, China) using bovine serum albumin (BSA) as standard.

For antibody production, healthy rabbits weighing 2.5kg were immunized by subcutaneous injection with 400μg *Tc*-SOD protein mixed with an equal volume of adjuvant at a 2-week interval (Freund's complete and incomplete adjuvant for the subsequent three immunizations). Serum antibody titres were monitored by indirect ELISA, with antigenicity confirmed through Western blot analysis. Every experiment was repeated three times.

Western blot analysis: The recombinant SOD protein was transferred to PVDF membrane (Millipore, USA) as

In Press

previously described (Li *et al*., 2021; Zhou *et al*., 2022). The rabbit anti-*Tc*-SOD polyclonal antibody diluted 1:8,000 was incubated at 4°C for 12-14h (anti-*Tc*-SOD antibody was purified in advance with A+G Agarose) (Beyotime, Shanghai, China). Finally, the strips were incubated with goat anti-rabbit IgG antibody (1:5,000) for 1h, and the images were visualized using a luminescence imaging system (Tanon, Shanghai, China).

qRT-PCR: Total RNA was extracted from the *T. canis* and its tissues, including reproductive organs (e.g., ovary, uterus, seminal vesicles, testis), intestines, body wall, and muscles by the Trizol method. The concentrations and purities of the total RNA were assessed using a NanoDrop spectrophotometer (Thermo Fisher Scientific, MA, USA), and reverse transcribed to cDNA as previously described. The mRNA transcription levels of *Tc-sod* in *T. canis* and its tissues were analyzed using qRT-PCR. A Light Cycler® 96 System (Roche, Switzerland) was used for qRT-PCR analysis, and the procedure was as follows: 95℃ for 30s and 95℃ for 5s, 60℃ for 30s, for a total of 40 cycles. Relative transcription levels of the *Tc-sod* gene were calculated using the $2^{-\triangle\triangle CT}$ method (Livak and Schmittgen, 2001), with 18S rRNA as the internal reference gene. The primer sequences used in this study are listed in Table 1. Each experiment was repeated three times.

Indirect immunofluorescence assay (IFA): Fixed *T. canis* with 4% paraformaldehyde for 48h, and then embedded it in paraffin blocks. Used a slicer to cut the tissue into 4μm sections and dried them at 65°C. These slices were soaked three times in xylene to remove paraffin, then rehydrated sequentially with ethanol (100, 95, and 85%) and finally in water. The sections were blocked with 5% BSA in PBS (pH 7.2) for 30min, then incubated with anti-*Tc*-SOD IgG (1:2000) at 4°C overnight, followed by incubation with FITC-conjugated goat anti-rabbit IgG (1:1000) at 37°C for 1h. Slices were washed three times with PBS and then incubated with 4,6-diamidino-2-phenylindole (DAPI) at room temperature in the dark for 5min, and observed under a Leica microscope (Leica, Germany). Each experiment was repeated three times.

Transfection of siRNA: The L3 larvae were washed with a sterile saline solution to remove excess impurities, following established protocols (Fu *et al*., 2014). The uptake of siRNA by *T. canis* was assessed using FAM-labelled (5′-carboxyfluorescein) control siRNA in RPMI-1640 medium containing 1% penicillin/streptomycin (Solarbio, Beijing, China). Electroporation was performed on the eggs and larvae using a Gene Pulser II System (Bio-Rad, USA) (1,000V, 200Ω, 24μF). Following co-incubation for 15min, the treated larvae and eggs were transferred to the RPMI-1640 culture medium in the CO_2 incubator for 24h. Fluorescence staining of the eggs and L3 larvae was subsequently observed under a fluorescence microscope.

RNAi: Three specific siRNA sequences targeting *Tc-sod* and one negative control siRNA sequence (with no homology to any *T. canis* sequence) were designed using the website-based tool siDirect 2.1 (https://sidirect2.rnai.jp/). These siRNA molecules were designated *Tc-sod*-siRNA-61, *Tc-sod*-siRNA-243, *Tc-sod*-siRNA-385, and NC-siRNA, which were tested and synthesized by Sangon Biotechnology (Shanghai, China). The siRNA was diluted with diethylpyrocarbonate (DEPC) treated water to 125μM and stored at -80°C for future use. The experiment was divided into five groups (*Tc-sod*-siRNA-61 group, *Tc-sod*-siRNA-243 group, *Tc-sod*-siRNA-385 group, NC-siRNA group, and PBS group).

T. canis were transferred to RPMI-1640 medium and treated with siRNA by the immersion method (Ma *et al*., 2019). The siRNA groups were treated with a concentration of 100nM *Tc-sod*-siRNA-61, *Tc-sod*-siRNA-243, *Tc-sod*-siRNA-385, and NC-siRNA, and cultured at 37℃ with 5% CO_2 for 12h and 24h, respectively. Thereafter, transcription levels of *Tc-sod* across the different groups were determined by qRT-PCR using specific primers (Table 1). For experimental condition optimization, *T. canis* were immersed in 100nM and 200nM *Tc-sod*-siRNA-61, respectively, and cultivated at 37°C under 5% CO_2 conditions for 24, 48, and 72h. The total RNA and protein of the *T. canis* were extracted at 72h post-interference, and the mRNA transcription and protein expression levels were analyzed using qRT-PCR and Western blot, respectively. The siRNA silence sequences are displayed in Table 2.

Table 1: Primer sequences used in the present study

Name	Sequence (5'-3')
q-Tc-sod-F	CTCCAACCGATAGCATAAGA
q-Tc-sod-R	ACAACTACTGAACGACCAAT
18S rRNA-F	AATTGTTGGTCTTCAACGAGGA
18S rRNA-R	AAAGGGCAGGGACGTAGTCAA

Table 2: *Tc-sod* specific siRNAs and control siRNAs used in the RNA interference assay

Name	Sequence
Tc-sod-siRNA-61-sense	AAGACCAAAUUCACAUUACTT
Tc-sod-siRNA-61-antisense	GUAAUGUGAAUUUGGUCUUTT
Tc-sod-siRNA-243-sense	UAGCAUUUCCGACAAGCAUTT
Tc-sod-siRNA-243-antisense	AUGCUUGUCGGAAAUGCUATT
Tc-sod-siRNA-385-sense	UACAUCAAUACGGUGAUACTT
Tc-sod-siRNA-385-antisense	GUAUCACCGUAUUGAUGUATT
Negative control-sense	UUCUCCGAACGUGUCACGUTT

Treatment of eggs and larvae with *Tc-sod*-siRNA-61: *T. canis* eggs and larvae were transfected with 200nM *Tc-sod*-siRNA-61, while the NC-siRNA group and PBS group received NC-siRNA and sterile PBS, respectively. The eggs were incubated under sterile conditions at 30℃ in a final volume of 3mL, with counts performed every 24h over 7 days. The proportion of eggs exhibiting normal development (the eggs in the stage of egg cell differentiation and development) and restricted development (where the differentiation of egg cells was limited and incomplete) was calculated, analyzed and a curve was drawn based on the developmental ratios. Finally, the phenotypic changes of eggs and larvae after interference (72h) were observed and recorded under an optical microscope.

Infection of mice with treated eggs: To evaluate the survival rate and pathogenicity of larvae treated with *Tc-sod*-siRNA-61, 45 mice were divided into 3 groups (*Tc-sod*-siRNA-61 group, NC-siRNA group, and PBS group, with 15 mice in each group). Subsequently, 3,000 eggs transfected with *Tc-sod*-siRNA-61 / NC-siRNA, or treated with PBS, were orally administered to each group

In Press

of mice, respectively. The health status of the mice was monitored daily, and mice were euthanized at 7dpi. The liver, lungs, and brain tissues from 6 mice were sectioned into fragments, and larvae were collected by artificial gastric juice digestion (consisting of 1% pepsin and 1% HCl in water at 37°C for 4-5h) (Healy *et al*., 2022). The larvae load was assessed, and each sample was counted 10 times.

The liver, lungs, and brain tissues from 6 mice were separated and fixed with 4% paraformaldehyde, as previously described. Subsequently, the tissue sections were stained with hematoxylin and eosin (H.E.), and histopathological changes were observed under a light microscope. Finally, according to the scoring criteria (Fan *et al*., 2003) and light microscope images, the inflammatory damage and pathological changes in the samples were scored by three individuals who were blinded to the mice group assignments.

Statistical analysis: All statistical analyses of the data were performed using GraphPad Prism 8.0 software (GraphPad Software, San Diego, CA, USA) and are expressed as the mean ±SD. Experiments were performed independently in triplicate. Student's *t*-test and ANOVA were used to analyze the differences among groups. When the *P*-values were less than 0.05, the difference was considered statistically significant. "ns" stands for no significant difference.

RESULTS

Characterization and structure analysis of *Tc-sod*: The coding sequence of *Tc-sod* was 573 bp in length and encoded 190 amino acids. *Tc-sod* contained a signal peptide, a transmembrane domain, and the SOD domain (Fig. 1A, B) (Supplementary Fig. S1). *Tc-sod* showed a highly significant similarity of 80.79% with *Ov*-SOD of *O.volvulus* (Genbank accession no. P24706.1) and 79.87% with *Brugia malayi* (Genbank accession no. AAR06638.1). The secondary structure shows that the *Tc*-SOD protein comprises 14.74% α-helix, 24.21% extended strand, 6.84% β-turn, and 54.21% random coil elements. The homology modeling was further used to construct the predicted three-dimensional structures of the SOD protein. The Ramachandran plots revealed that 90.81% of residues were in favored regions, 97.84% of residues were in allowed regions, while only 2.16% of residues were in outlier regions, suggesting the validity of the *Tc-sod* model (Supplementary Fig. S2).

Tc-sod contained the potential Cu^{2+} binding sites (H78, H80, H95, and H152), the Zn^{2+} binding sites (H95, H103, H112, and D115), enzyme active sites (H95 and R178), and the SOD signature sequence (Fig. 1C, D). There were two cysteine residues (Cys-89 and Cys-181) in this sequence, which are key factors in the formation of disulfide bonds in *Tc-sod* (Fig. 1E). GO analysis further indicated roles in metal ion binding and extracellular superoxide scavenging.

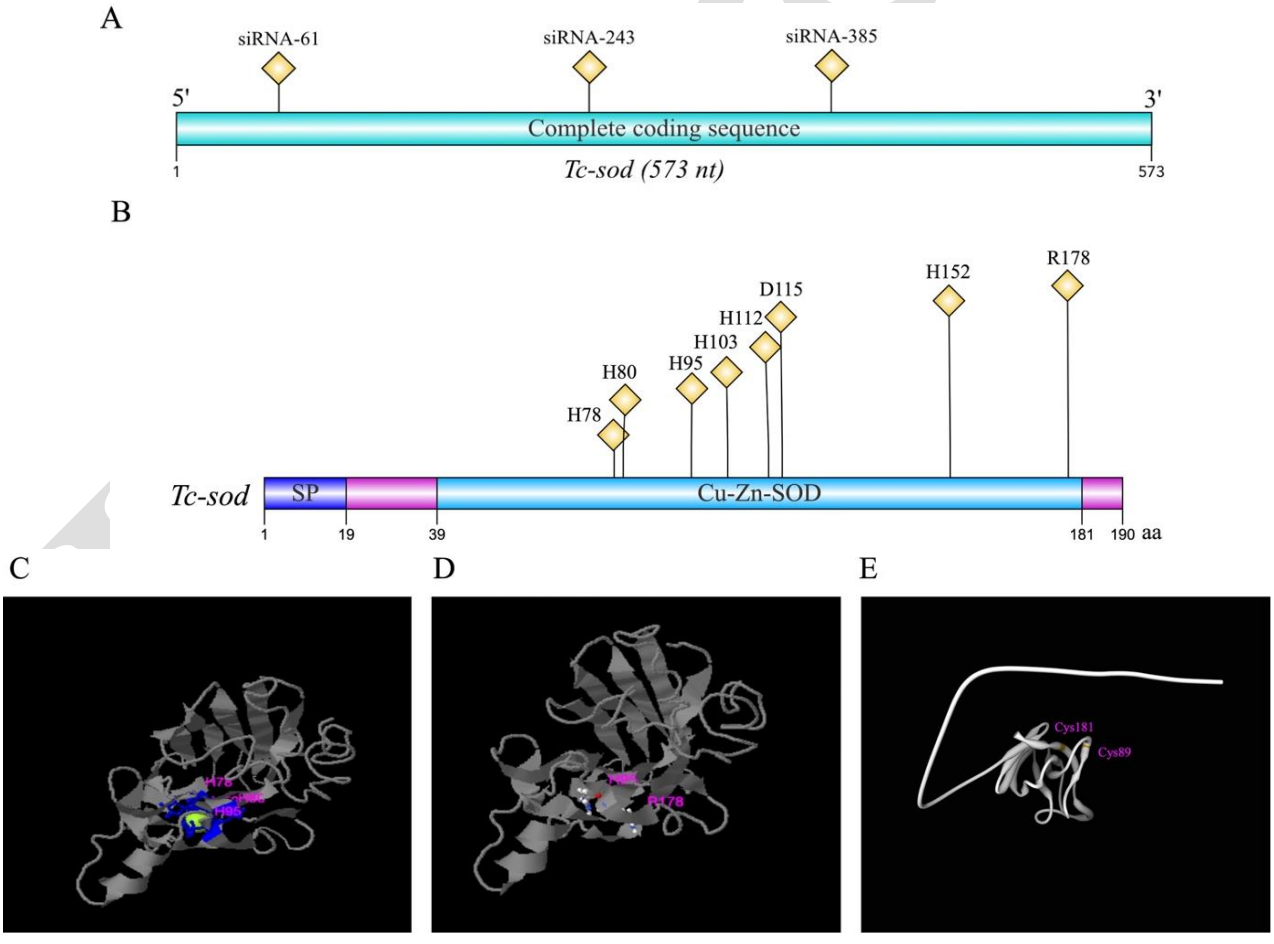

Fig. 1: Characterization of the *Tc-sod* gene from *T. canis*. (A) Complete coding sequence of *Tc-sod*. (B) Amino acid sequence and functional domain prediction of *T. canis Tc-sod* (190 aa). (C-D) It represents the Cu^{2+} and Zn^{2+} ion binding sites and active sites. (E) Two cysteine residues are shown at Cys-89 and Cys-181.

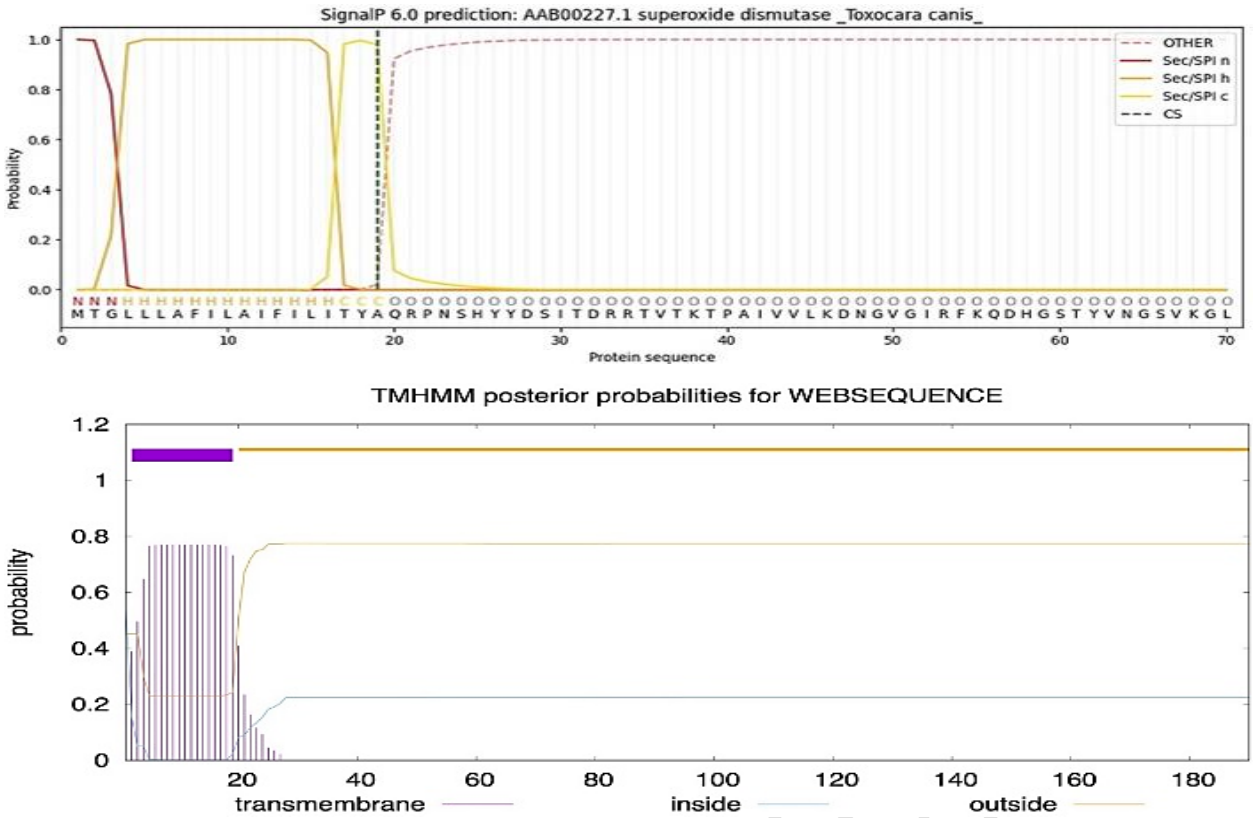

Supplementary Fig S1: (A) Signal peptide prediction of *Tc-sod.* Thehydrophobic signal peptide at the C-terminal. (B) Transmembrane region prediction of *Tc-sod* (2-19). Note: Supplementary data associated with this article.

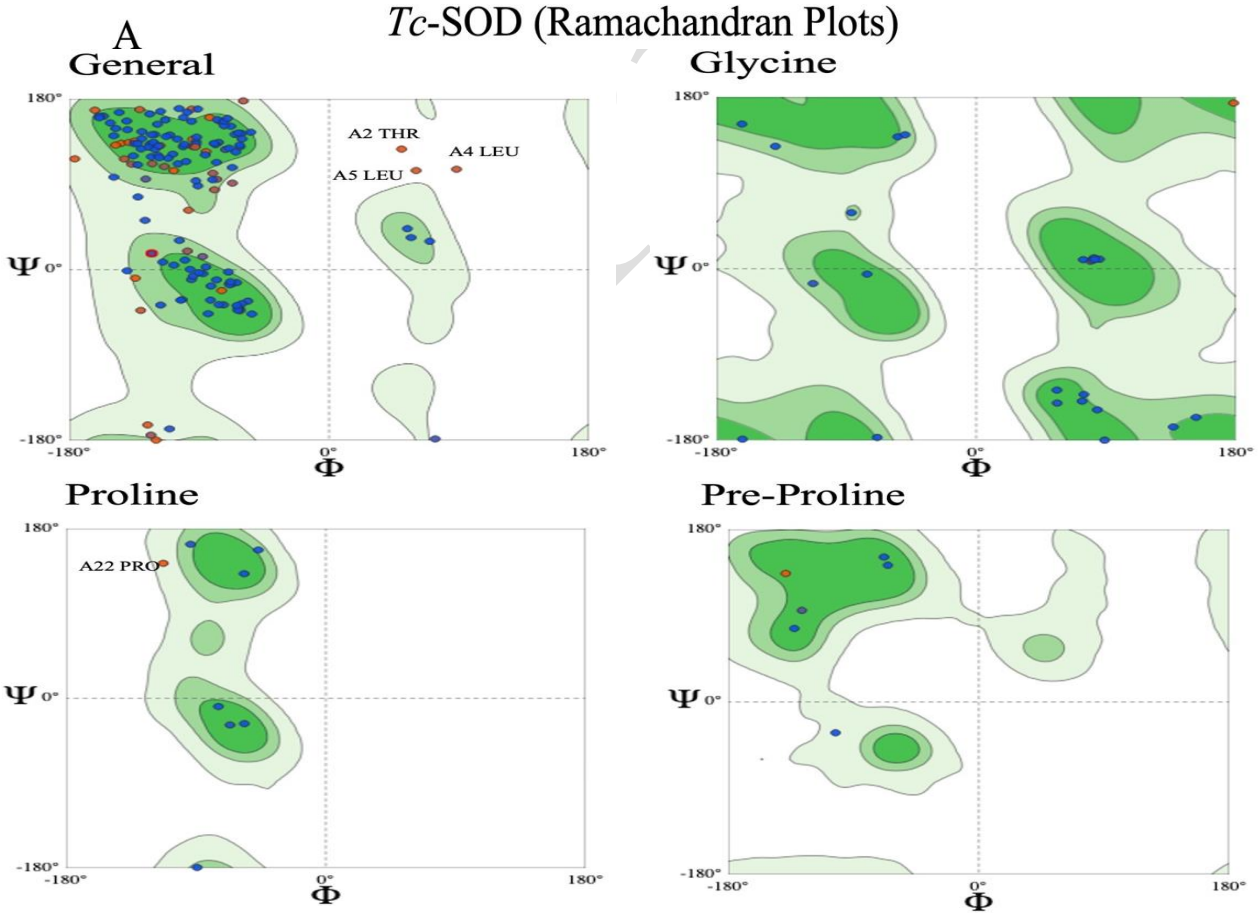

Supplementary Fig S2: Ramachandran Plots were determined for the homology structure model from *T. canis* SOD (*Tc*-SOD). 90.81% (168/185) of all residues were in favoured regions. 97.84% (181/185) of all residues were in allowed regions. There were 4 outliers (phi, psi): A2 THR (50.29, 127.06), A4 LEU (88.34, 105.81), A5 LEU (60.29, 104.42), A22 PRO (-112.66, 143.18). Note: Supplementary data associated with this article.

Identification and tissue expression of *Tc*-SOD: The *Tc*-SOD recombinant protein (with a size of 37kDa) demonstrated strong antigenicity and could be recognized by the host immune system, and the antibody titre reached more than 1:32,0000 after the third immunization (Fig. 2B, C). The transcription profiles of *Tc-sod* in the life stage of *T. canis* were compared using qRT-PCR, revealing differential levels at various stages of the *T. canis* life cycle (Fig. 2D). The *Tc-sod* transcription was observed in female, male, and L3 larvae of *T. canis*, and the mRNA transcription level in females was significantly higher than that in males and L3 larvae (P<0.01). The differences in *Tc-sod* transcription levels across various tissues were significant. The mRNA transcription level of *Tc-sod* was relatively abundant in reproductive (e.g., ovary and uterus) and intestinal tissues, and was considerably higher than that in muscle and body wall tissues (Fig. 2E, F). Indirect immunofluorescence histochemistry revealed that *Tc*-SOD was expressed in the uterus, ovary, and egg cells of female adults (Fig. 2G), as well as in the body wall of male adults.

siRNA delivery to *T. canis* larvae: The FAM-siRNA was transfected into L3 larvae by electroporation and immersion methods, and the fluorescence staining within the larvae was observed under a fluorescence microscope. The result showed that the fluorescence distribution of larvae treated with the immersion method (Fig. 3c, d) was stronger than that of the electroporation method. However, no fluorescence staining was observed in the untreated larvae (Fig. 3a, b), indicating that siRNA can be effectively delivered to *T. canis* through the immersion method.

***Tc-sod* mRNA transcription level after silencing the *Tc-sod* gene:** The qRT-PCR results showed that the mRNA transcription levels of the *Tc-sod*-siRNA-61 and *Tc-sod*-siRNA-243 groups were decreased by 55.05% and 39.86%, respectively. After 24h of interference, the mRNA transcription levels of *Tc-sod*-siRNA-61 and *Tc-sod*-siRNA-243 groups were suppressed by 62.94% and 60.05%, respectively (P<0.01). However, no significant inhibition occurred with NC-siRNA or *Tc-sod*-siRNA-385 on *Tc-sod* mRNA transcription (Fig. 4A).

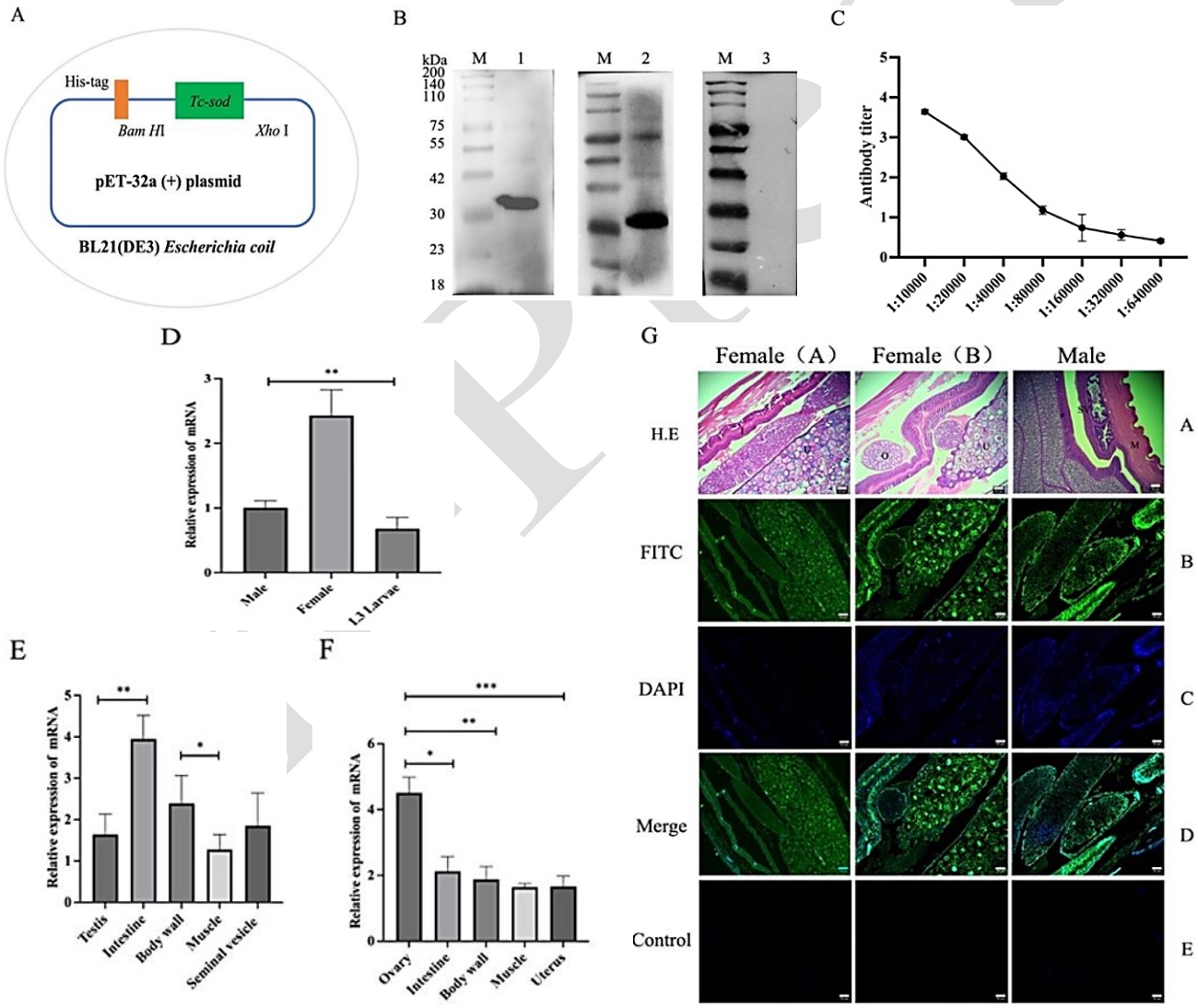

Fig. 2: Identification of *Tc*-SOD protein antigenicity and expression pattern. (A). Schematic diagram of pET-32a (+)-*Tc-sod* prokaryotic expression vector construction. (B). M: Protein Marker, Lane 1. Western blot of canine positive serum binding to *Tc*-SOD protein; lane 2. Western blot of mice positive serum binding to *Tc*-SOD protein; lane 3. Western blot of negative serum binding to *Tc*-SOD protein. (C). Titer determination of polyclonal antibodies after the final immunization was measured by indirect ELISA. (D-F). The mRNA transcription levels of *Tc-sod* in *T. canis* and tissues were assessed by qRT-PCR. (G). Tissue localization of *Tc*-SOD in *T. canis*. B: Body wall; U: Uterus; I: Intestine; O: Ovary. Scale bars = 50 μm. All the assays are performed as the mean ± SD of triplicate experiments. Statistically significant differences with * P<0.05, ** P<0.01, *** P<0.001, and **** P<0.0001.

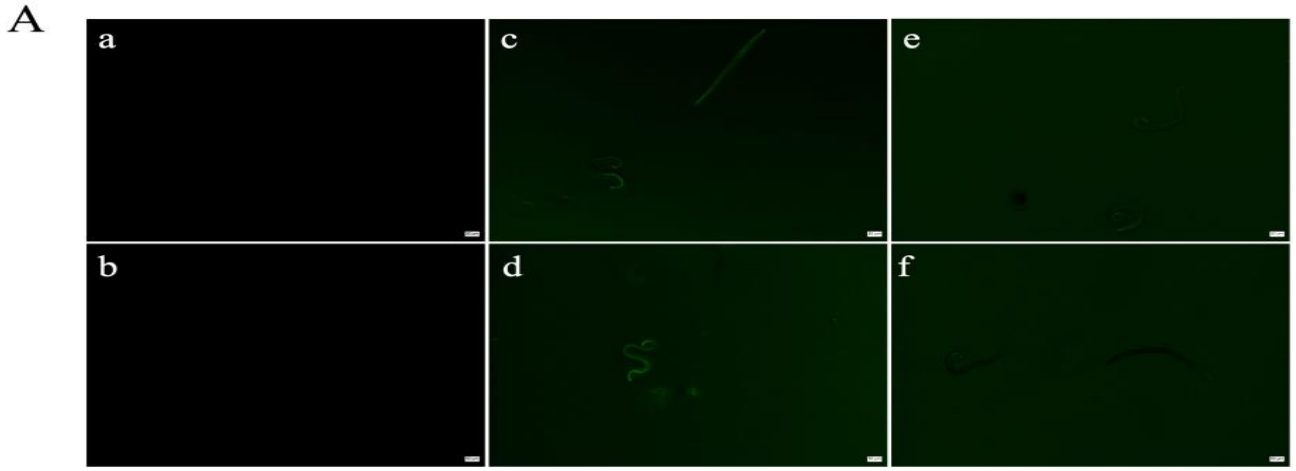

Fig. 3: Detection of siRNA delivery to *T. canis* larvae via fluorescence microscopy. (A). The FAM-siRNA delivery to *L3 larvae* and no fluorescence was observed in untreated L3 larvae. (a, b) Larvae untreated with FAM-siRNA. (c, d) larvae treated by immersion with FAM-siRNA. (e, f) treated by electroporation with FAM-siRNA. Scale bars = 50 μm.

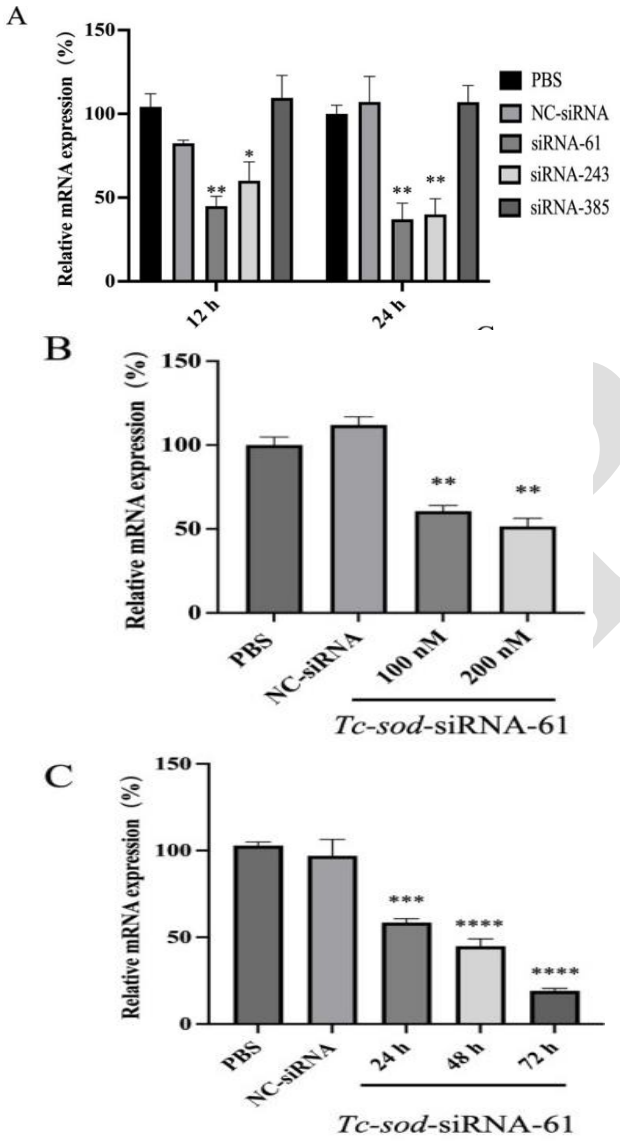

Fig. 4: Specific siRNA suppresses mRNA transcription levels of *Tc-sod*. (A). The mRNA transcription levels of *Tc-sod* in adult *T. canis* after treatment with different siRNAs. (B). treatment with 100 and 200 nmol/L *Tc-sod*-siRNA-61. (C). treatment with 200 nmol/L *Tc-sod*-siRNA-61 for 24 h, 48 h, and 72 h. All the assays are performed as the mean ± SD of triplicate experiments. Statistically significant differences with * P<0.05, ** P<0.01, *** P<0.001, and **** P<0.0001.

Dose-response studies revealed concentration-dependent silencing, where 100nM and 200nM *Tc-sod*-siRNA-61 decreased transcription levels by 39.36% and 49.39% (P<0.01), respectively, compared with the PBS group (P<0.01) (Fig. 4B). The results related to the efficacy of siRNA-mediated knockdown showed that the silencing efficiency achieved with 200nM *Tc-sod*-siRNA-61 was the optimal knockdown effect. Therefore, 200nM *Tc-sod*-siRNA-61 was used to optimize the working conditions. At this concentration, the mRNA transcription levels of *Tc-sod* decreased with the extension of interference time, by 41.46% (P<0.001), 52.8%, and 76.87% (P<0.0001) at 24, 48, and 72h, respectively (Fig. 4C).

***Tc-sod*-siRNA-61 inhibits the expression of *Tc*-SOD protein:** The *T. canis* was washed and cultured in medium with a final concentration of *Tc-sod*-siRNA-61 at 200nM for 72h. The mRNA transcription level and protein expression of *Tc-sod* were analyzed using qRT-PCR and Western blot, respectively under optimal interference conditions. The results revealed that compared with the PBS group, the mRNA transcription level of *Tc-sod* was reduced by 78.49% (P<0.001) (Fig. 5A), and the protein expression level of *Tc*-SOD was suppressed by 62.64% (P<0.01) (Fig. 5B). This silencing was effective, both at the mRNA transcription and protein expression levels.

The indirect immunofluorescence histochemistry demonstrated that the fluorescence staining of the uterus, body wall, and muscles of *T. canis* in the PBS and NC-siRNA groups was intense, indicating high expression of *Tc*-SOD protein. On the contrary, the fluorescence distribution in the *Tc-sod*-siRNA-61 group was significantly reduced (Fig. 5C, D) (P<0.05).

***Tc-sod* is essential for the growth and development of eggs and larvae:** Fluorescence distribution inside the eggs confirmed that the siRNA can be transferred into the eggs through the immersion method (Fig. 6A). Regarding development and morphology of eggs, the proportion of eggs with developmental inhibition and defects in the *Tc-sod*-siRNA-61 group noticeably increased (P<0.01), compared to the PBS group. Concurrently, the egg hatching rates were markedly reduced in the *Tc-sod*-siRNA-61 group (P<0.05) (Fig. 6B-E). As shown in Fig. 6F,

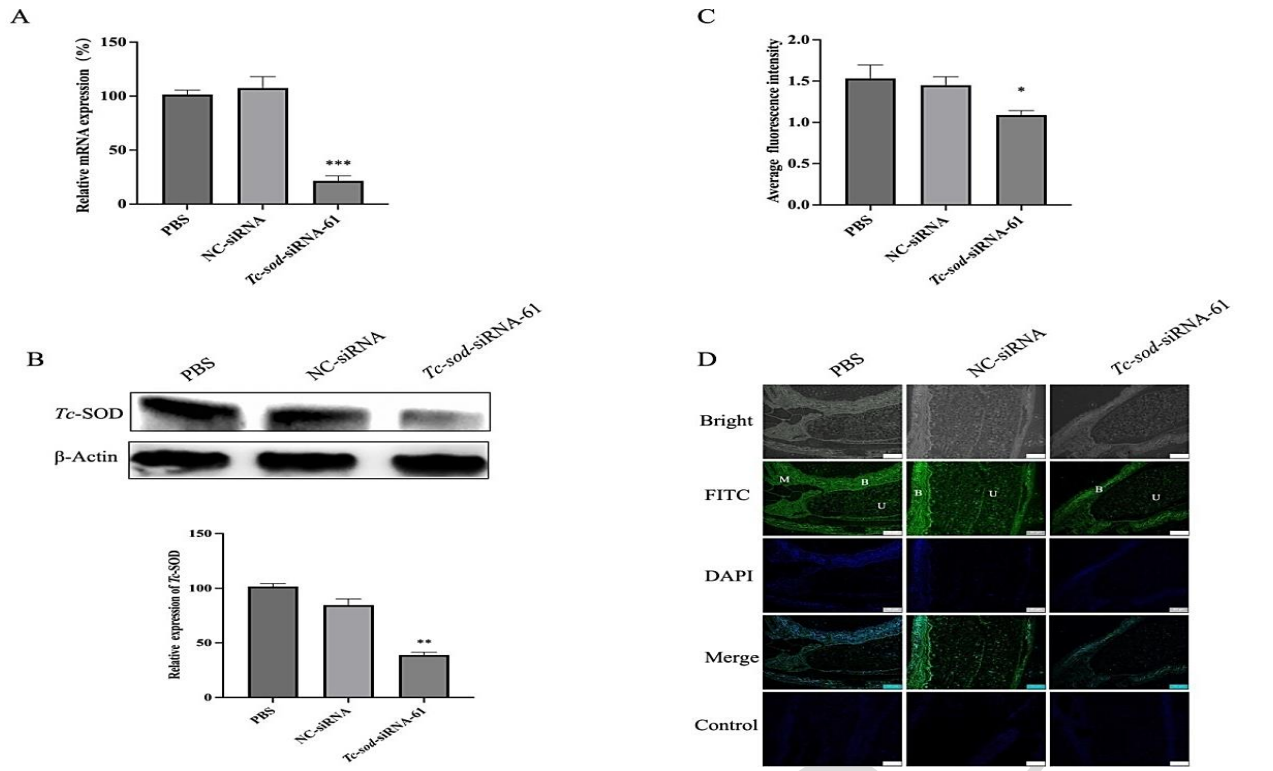

Fig. 5: *Tc-sod*-siRNA-61 inhibits the transcription and expression of *Tc-sod*. (A). qRT-PCR and (B) Western blot analysis of relative mRNA transcription levels and protein expression of *Tc-sod* under optimal interference conditions. (C). The immunofluorescence signal was analyzed with Image J. (D). The *T. canis* sections were detected using anti-*Tc*-SOD serum, while normal serum was used as a negative control. *T. canis* were stained with FITC (green) and DAPI (blue). Strong immune staining was observed of *T. canis* in the PBS and NC-siRNA groups, while the fluorescence signal in the *Tc-sod*-siRNA-61 group was weak. U: Uterus; B: Body wall; M: Muscle. Scale bars = 50 μm. All the assays are performed as the mean ± SD of triplicate experiments. Statistically significant differences with * P<0.05, ** P<0.01, *** P<0.001, and **** P<0.0001.

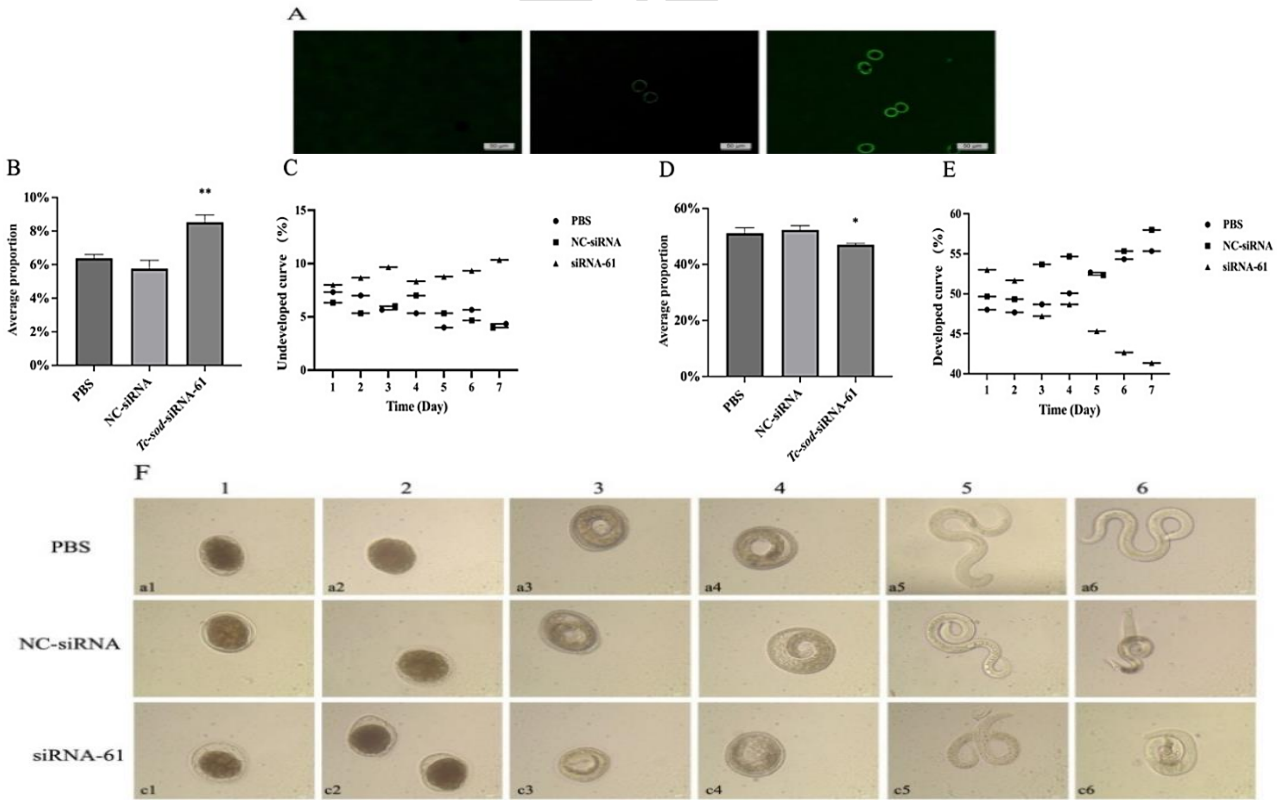

Fig. 6: The silencing of *Tc-sod* affects the activity and developmental status of eggs. (A). The FAM-siRNA was transfected into the eggs; (a) Eggs without FAM-siRNA transfection. (b-c) Eggs treated by immersion with FAM-siRNA. Scale bars = 50 μm. (B-C) The proportion and curve of inhibition and unhatched eggs. (D-E) The proportion and curve of hatching eggs. (F) The phenotypic changes were recorded by a microscope. (a1-a8) PBS group; (b1-b8) NC-siRNA group; (c1-c8) *Tc-sod*-siRNA-61 group, showing detachment of damaged cuticle. (1-2) Eggs hatching; (3-4) Infective eggs; (5-6) L3 larvae. Images were taken at 40 x magnification. All the assays are performed as the mean ± SD of triplicate experiments. Statistically significant differences with * P<0.05, ** P<0.01, *** P<0.001, and **** P<0.0001.

developmental defects of eggs, increasing gaps between embryonic cells, and larvae deformities were observed in the *Tc-sod*-siRNA-61 group, while larvae displayed cuticular defects, motility impairment, and reduced flexibility and extensibility.

***Tc-sod* reduces the larvae burden in infected mice:** To investigate whether *Tc-sod*-siRNA-61 mediated phenotypic changes, affecting parasite survival in the host, mice were orally infected with treated eggs. Compared with the PBS group, the larvae reduction rate of the *Tc-sod*-siRNA-61 group was 33.4% (P<0.05) (Fig. 7), indicating that the motility of the larvae was inhibited. Nevertheless, there was no significant change in the larvae burden observed in the NC-siRNA group.

***Tc-sod* is significant for *T. canis* infection and invasion:** Gross and histopathological analyses were performed on the mice liver, lung, and brain tissues. In the PBS and NC-siRNA groups, hepatic morphology showed significant alterations, with edema and degeneration of hepatocytes, and showed a severe inflammatory infiltration composed of eosinophils and neutrophils (Fig. 8B). By contrast, the mice

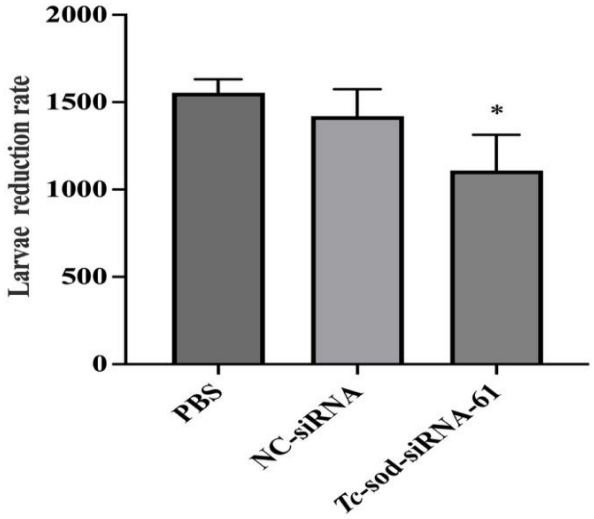

Fig. 7: *Tc-sod* is essential for the growth and survival of *T. canis*. The larvae reduction rate of mice at 7 dpi, the mice of groups treated with PBS, NC-siRNA, and siRNA-61 were humanely euthanized. All the assays are performed as the mean ± SD of triplicate experiments. Statistically significant differences with * P<0.05, ** P<0.01, *** P<0.001, and **** P<0.0001.

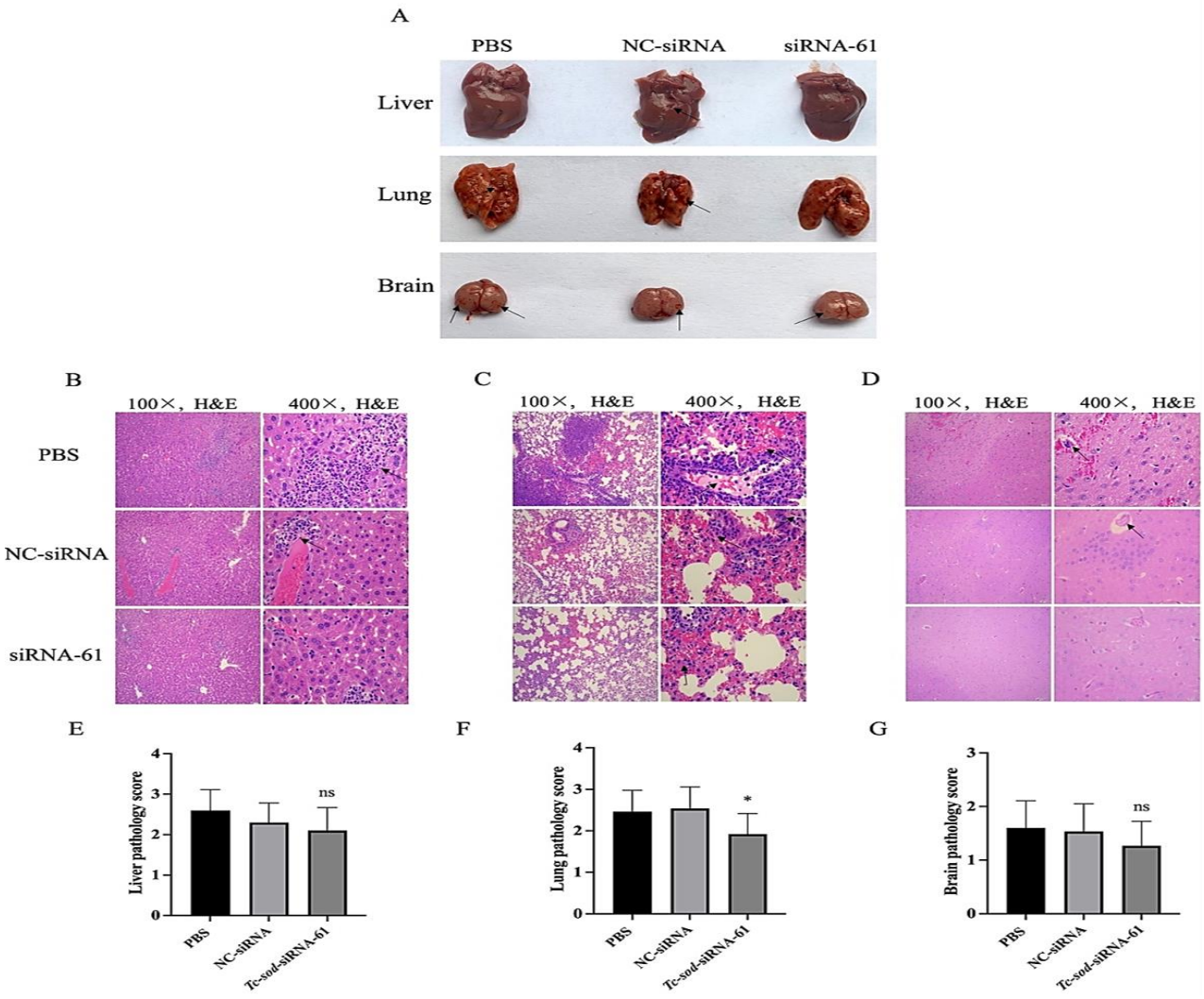

Fig. 8: *Tc-sod*-siRNA-61 alleviate the pathogenicity of *T. canis* to host tissues. (A). Gross pathological changes in the liver, lungs, and brain were examined at 7 dpi, with black arrows denoting prominent larvae migratory traces. (B) liver, (C) lungs, and (D) brain tissues of mice were stained with hematoxylin and eosin (H&E), and the histopathological changes were observed under an optical microscope. Scale bars = 50 µm. (E-G) Average histopathological lesion scores; D: liver; E: lungs; F: brain. Three observers scored the tissues damage without a clear grouping of mice. Statistically significant differences with * P<0.05, ** P<0.01, *** P<0.001, and **** P<0.0001.

in the *Tc-sod*-siRNA-61 group only showed mild local inflammatory infiltration and nuclear morphological changes.

Lung pathology revealed marked lesions in the PBS and NC-siRNA groups, characterized by many red blood cells extravasation, and perivascular inflammation was mainly characterized by inflammatory infiltration of eosinophils, lymphocytes, and neutrophils. The interstitial space around the blood vessels was widened, and there was exudate accumulated in the alveolar cavity (Fig. 8C). Nevertheless, compared with the control group, mice in the *Tc-sod*-siRNA-61 group exhibited minor pneumonia, haemorrhagic lesions, inflammatory cell infiltration, and pulmonary membrane degeneration.

In brain tissues, both PBS and NC-siRNA groups showed red blood cells and varying numbers of inflammatory cells (eosinophils and lymphocytes), while only showing slight haemorrhagic lesions and inflammatory reactions in the *Tc-sod*-siRNA-61 group (Fig. 8D). In addition, the surface of the cerebral cortex in the brain tissue of mice in each group showed spotty bleeding lesions and obvious traces of migration, with the lesions being relatively less serve in the *Tc*-sod-siRNA-61.

The histopathological damage score based on inflammatory cell infiltration and tissue degeneration showed that merely mild to moderate inflammatory damage in the tissues of mice in the *Tc-sod*-siRNA-61 group, especially in the lungs (Fig. 8E-G) (mean injury index: $P<0.05$).

DISCUSSION

Superoxide dismutase, as the primary barrier of the antioxidant system, plays multiple effector functions in the oxidative defense of organisms, such as maintaining parasite proliferation, replication, and survival (Fernández-García *et al*., 2013; Yuan *et al*., 2019; Motavallihaghi *et al*., 2022). These characteristics facilitate the parasite to exert its ability to eliminate various harmful reactive products, especially during infection. Therefore, exploring the expression of SOD in the *T. canis* and its developmental stages is a prerequisite for understanding the role of this protein. Here in this study, the expression of the SOD was detected in the egg and larval stages as well as in the reproductive organs, body wall, and musculature of the *T. canis*. The expression profiling and immunolocalization study suggested that *Tc*-SOD may be related to the development and growth of *T. canis*. Localization of the SOD in *T. canis* contrasts sharply with the localization of SOD in *Angiostrongylus cantonensis* and *Fasciola hepatica* (Yuan *et al*., 2019; Calvani *et al*., 2022), which may be related to different parasite species and life cycle characteristics. However, in all three types of parasites, immune localization occurs on the parasite's surface, supporting the postulate that the worms utilize SOD to defend against superoxide damage. *Sod* has been detected in both the larvae and adult stages of *T. solium* and *S. erinacei*, suggesting its importance in the physiological processes and life cycle of the parasites (Castellanos-González *et al*., 2002; Vaca-Paniagua *et al*., 2008; Li *et al*., 2010).

Earlier studies in *T. canis* have shown that transfection by immersion could inhibit gene expression of *Tc*-PP1cα and *Tc*-AQP-1 and decrease the reproductive and drug transport abilities in *T. canis* (Ma *et al*., 2015; Ma *et al*., 2019). By contrast, in *Trichostrongylus colubriformis* and *Litomosoides sigmodontis,* transfection by electroporation was found to be more efficient than immersion (Issa *et al*., 2005; Pfarr *et al*., 2006). Three siRNAs (si-61, si-243, and si-385), targeting three different positions in the *Tc-sod* transcript, were designed. The immersion method was found to exhibit higher efficiency in transfecting siRNA and successfully inhibited the mRNA transcription and expression of the SOD protein. It is worth noting that other SODs exist in the genome database of *T. canis*, and the nucleotide sequences of these SODs may have some degree of homology with Cu/Zn-SOD. However, here, initial studies of the role of SOD in *T. canis* did not distinguish between the Cu/Zn-SOD and other isoforms. In this study, by detecting the transcription and translation levels of *Tc*-SOD, we demonstrated that the downregulation of SOD activity and functional effects can be attributed to the inhibition of Cu/Zn SOD. The reason is that previous sequence analysis showed that low nucleotide homology between Cu/Zn-SOD and other isoforms, particularly within the siRNA-targeted region, which substantially reduces the possibility of SOD interference effects (cross-silencing) accumulating. Of course, considering the direction of future research, specific siRNA targeting different SODs should be designed to analyze the role of SOD isoforms more accurately in the pathogenicity and survival of *T. canis*.

Phenotypic analysis is considered a key indicator for assessing the effectiveness of RNAi and for investigating the specific role of genes in the life activities of a parasite. In this study, delayed egg hatching and an increase in the proportion of morphologically abnormal eggs upon *Tc-sod* silencing were observed. The eggs and larvae of the *Tc-sod*-siRNA-61 group exhibited developmental disorders and abnormal morphology, characterized by increased eggshell space and cuticle damage. The cuticle, a critical host-parasite interface, mediates the absorption of nutrients, the secretion of substances, osmotic regulation, cell protection, and the host immune response process. Here, these defects likely result from a compromised SOD-mediated oxidative defense, leading to disruption of the cuticle structures and cellular / tissue integrity in *T. canis*, which further affected the survival of larvae. Extracellular SOD has been reported to not only participate in the clearance of reactive oxygen species but is also related to the apoptosis of epidermal cells (Amstad *et al*., 1991). In *Caenorhabditis elegans* and mosquito *Culex pipiens*, activating the expression of SOD-3 prolongs the survival period of nematodes, while inhibiting SOD-2 shortens the survival time of adult mosquitoes (Sim *et al*., 2011; Zimmerman *et al*., 2014). These studies indicate that inhibition of SOD can affect the survival cycle of parasites and insects, as well as the integrity of the cell epidermis.

Phenotypic changes observed *in vitro* may lead to the clearance of *T. canis* in vivo, which combined with these RNAi-induced effects and the host immune response, could impair the worm's ability to withstand host-induced oxidative or immunological stress. Here, suppressing *Tc-sod* remarkably reduced larvae burden in infected mice. Yuan *et al*. (2019) found that *A. cantonensis* SOD-3 was closely related to the survival rate of larvae, and its high

expression can reduce the oxidative damage in larvae. Considering that *Tc-sod* gene silencing could weaken the growth and survival of larvae, this intervention may further influence the pathogenicity of larvae toward host tissues. Notably, the invasion efficiency of larvae and the degree of tissue lesions in mice were significantly reduced when *Tc-sod* was blocked in the present study. This situation is similar to that of *Leishmania*, where the deficiency of SOD significantly affects the survival rate and replication of the parasites in macrophages, weakening its pathogenic ability to the skin (Mittra *et al*., 2017). SOD has been postulated to play a role in adapting the microbes to the internal environment of the host and is essential in microbial survival and virulence (Pratt *et al*., 2015; Mittra *et al*., 2017; Schatzman and Culotta, 2018). Combining the perspectives of RNAi and immune prevention (Unpublished data), the possibility of *Tc-sod* as the target candidate against *T. canis* infection and treatment strategies warrants further investigation. The functional diversity of SOD is crucial for parasite survival, and further studies on SOD protein in *T.canis* are required to understand the critical role played by the protein in the development and survival of the parasite in different host tissues during its parasitic phase of the life cycle.

Conclusions: *T. canis* SOD was successfully silenced both at the transcriptional and protein levels in this study. This study suggests that the *Tc*-SOD protein may be involved in the reproductive and growth processes of the parasite. These findings highlight the functional diversity of *Tc-sod*, which has the potential to serve as a drug target and as an intervention measure for preventing *T. canis* infection.

Author contribution: Tian-LeWu: Writing—original draft, Methodology, Investigation, Conceptualizatio n.Bing-Nan Wang:Software, Validation. Bin-Yu Li: Investigation, Data curation.Zi-Ying Hu : Data curation, Validation. Yi-Ning You: Methodology, Data curation. Yong-Li Luo: Validation, Formal analysis. Shi-Cheng Bi: Funding acquisition, Conceptualization. Rong-Qiong Zhou: Writing—review & editing, Supervision, Project administration, Conceptualization.

Completing interests: The authors declare that they have no competing interests.

Ethics statement: All experiments involving animals were conducted following the guidelines of the Care and Use of Laboratory Animals of the Ministry of Science and Technology of the People's Republic of China (2006398). The animal procedures were approved and supervised by the Institutional Animal Care and Use Committee (IACUC) of Southwest University, China (Permit number: IACUC-20240806-02).

Fundings: This work was supported by the National Natural Science Foundation of China (No. 32473075) and Science and Technology Research Project of Chongqing Municipal Education Commission *(KJQN-202203504)*.

REFERENCES

Abou-El-Naga IF and Mogahed NMFH, 2023. Potential roles of *Toxocara canis* larval excretory-secretory molecules in immunomodulation and immune evasion. Acta Trop 238:106784. https://doi.org/10.1016/j.actatropica.2022.106784.

Amstad P, Peskin A, Shah G, *et al*., 1991. The balance between Cu, Zn-superoxide dismutase and catalase affects the sensitivity of mouse epidermal cells to oxidative stress. Biochem 30(38):9305-9313. https://doi.org/10.1021/bi00102a024.

Auer H and Walochnik J, 2020. Toxocariasis and the clinical spectrum. Adv Parasitol 109:111-130. https://doi.org/0.1016/bs.apar.2020.01.005

Borgstahl GEO and Oberley-Deegan RE, 2018. Superoxide Dismutases (SODs) and SOD Mimetics. Antioxidants 7:156. https://doi.org/10.3390/antiox7110156.

Bowman DD, 2021. *Ascaris* and *Toxocara* as foodborne and waterborne pathogens. Res Vet Sci 135:1-7. https://doi.org/10.1016/j.rvsc.2020.12.017

Broxton CN and Culotta VC, 2016. SOD Enzymes and Microbial Pathogens: Surviving the Oxidative Storm of Infection. PLoS Pathog 12:e1005295. https//doi.org/10.1371/journal.ppat.1005295.

Calvani NED, DeMarcoVerissimo C, Jewhurst HL, *et al*., 2022. Two Distinct Superoxidase Dismutases (SOD) Secreted by the Helminth Parasite *Fasciola hepatica* Play Roles in Defence against Metabolic and Host Immune Cell-Derived Reactive Oxygen Species (ROS) during Growth and Development. Antioxidants 11:1968. https://doi.org/10.3390/antiox11101968.

Cardoso RM, Silva CH, Ulian de Araújo AP, *et al*., 2004. Structure of the cytosolic Cu, Zn superoxide dismutase from *Schistosoma mansoni*. Acta Crystallogr D Biol Crystallogr 60(Pt 9):1569-1578. https://doi.org/10.1107/S0907444904016798.

Castellanos-González A, Jiménez L, Landa A, *et al*., 2002. Cloning, production and characterisation of a recombinant Cu/Zn superoxide dismutase from *Taenia solium*. Int J Parasitol 32:1175-1182. https://doi.org/10.1016/s0020-7519(02)00093-0.

ChenJ, Liu Q, LiuGH, *et al*., 2018. Toxocariasis: a silent threat with a progressive public health impact. Infect Dis Poverty 7:59. https://doi.org/10.1186/s40249-018-0437-0.

Crowe J, Lumb FE, Harnett MM, *et al*., 2017. Parasite excretory-secretory products and their effects on metabolic syndrome. Parasite Immunol 39(5):10. https://doi.org/10.1111/pim.12410

Da Silva MB, UrregoAJR, Oviedo Y, *et al*., 2018. The somatic proteins of *Toxocara canis* larvae and excretory-secretory products revealed by proteomics. Vet Parasitol 259:25-34. https://doi.org/10.1016/j.vetpar.2018.06.015.

Fan CK, Lin YH, Du WY, *et al*., 2003. Infectivity and pathogenicity of 14-month-cultured embryonated eggs of *Toxocara canis* in mice. Vet Parasitol 113:145-155. https://doi.org/10.1016/s0304-4017(03)00046-3.

Fava NMN, Cury MC, Santos HA, *et al*., 2020. Phylogenetic relationships among *Toxocara* spp. and Toxascaris sp. from different regions of the world. Vet Parasitol 282:109133. https://doi.org/10.1016/j.vetpar.2020.109133.

Fernández-García A, Alvarez-García G, Marugán-Hernández V, *et al*., 2013. Identification of *Besnoitia besnoiti* proteins that showed differences in abundance between tachyzoite and bradyzoite stages by difference gel electrophoresis. Parasitol 140:999-1008. https://doi.org/10.1017/S003118201300036X.

Fu CJ, Chuang TW, Lin HS, *et al*., 2014. Seroepidemiology of *Toxocara canis* infection among primary schoolchildren in the capital area of the Republic of the Marshall Islands. BMC Infect Dis 15:14:261. https://doi.org/10.1186/1471-2334-14-261.

Healy SR, Morgan ER, Prada JM, *et al*., 2022. Brain food: rethinking food-borne toxocariasis. Parasitol 149(1):1-9. https://doi.org/10.1017/S0031182021001591.

Healy SR, Morgan ER, Prada JM, *et al*., 2023. From fox to fork? *Toxocara* contamination of spinach grown in the south of England, UK. Parasit Vectors 16(1):49. https://doi.org/10.1186/s13071-023-05674-8.

Issa Z, Grant WN, Stasiuk S, *et al*., 2005. Development of methods for RNA interference in the sheep gastrointestinal parasite, *Trichostrongylus colubriformis*. Int J Parasitol 35:935-940. https://doi.org/10.1016/j.ijpara.2005.06.001.

Jaikua W, Kueakhai P, Chaithirayanon K, *et al*., 2016. Cytosolic superoxide dismutase can provide protection against *Fasciola gigantica*. Acta Trop 162:75-82. https://doi.org/ 10.1016/j.actatropica.2016.06.020.

Khouri R, Bafica A, Silva Mda P, *et al*., 2009. IFN-beta impairs superoxide-dependent parasite killing in human macrophages: evidence for a deleterious role of SOD1 in cutaneous leishmaniasis. J Immunol 182(4):2525-2531. https://doi.org/ jimmunol.0802860.

Lalrinkima H, Raina OK, Chandra D, *et al*.,2015. Isolation and characterization of Cu/Zn-superoxide dismutase in *Fasciola gigantica*. Exp Parasitol 151-152:1-7. https://doi.org/10.1016/j.exppara.2015.01.014.

Li AH, Na BK, Ahn SK, *et al*., 2010. Functional expression and characterization of a cytosolic copper/zinc-superoxide dismutase of *Spirometra erinacei*. Parasitol Res 106:627-635. https://doi.org/10.1007/s00436-009-1714-4.

Li F, Li XL, Chen SJ, *et al*., 2021. Excretory/secretory proteins of adult *Toxocara canis* induce changes in the expression of proteins involved in the NOD1-RIP2-NF-κB pathway and modulate cytokine production in mouse macrophages. Exp Parasitol 229: 108152. https://doi.org/10.1016/j.exppara.2021.108152.

Liu Y, Cao A, Li Y, *et al*., 2017. Immunization with a DNA vaccine encoding *Toxoplasma gondii* Superoxide dismutase (*Tg*SOD) induces partial immune protection against acute toxoplasmosis in BALB/c mice. BMC Infect Dis 17:403. https://doi.org/10.1186/s12879-017-2507-5.

Livak KJ and Schmittgen TD, 2001. Analysis of relative gene expression data using real-time quantitative PCR and the 2(-Delta Delta C(T)) Method. Methods 25:402-408. https://doi.org/10.1006/meth.2001.1262

Lopez-Alamillo S, Padyala P, Carey M, *et al*., 2025. Human toxocariasis. Clin Microbiol Rev e00101-23. https://doi.org/10.1128/cmr.00101-23

Ma GX, Zhou RQ, Song ZH, *et al*., 2015. Molecular mechanism of serine/threonine protein phosphatase 1 (PP1cα-PP1r7) in spermatogenesis of *Toxocara canis.* Acta Trop 149:148-154. https://doi.org/10.1016/j.actatropica.2015.05.026.

Ma G, Luo Y, Zhu H, *et al*., 2016. MicroRNAs of *Toxocara canis* and their predicted functional roles. Parasit Vectors 9:229. https://doi.org/10.1186/s13071-016-1508-3.

Ma G, Holland CV, Wang T, *et al*., 2018. Human toxocariasis. Lancet Infect Dis 18:e14-e24. https://doi.org/10.1016/S1473-3099(17)30331-6.

Ma G, Jiang A, Luo Y, *et al*., 2019. Aquaporin 1 is located on the intestinal basolateral membrane in *Toxocara canis* and might play a role in drug uptake. Parasit Vectors. 12: 243. http://doi.org/10.1186/s13071-019-3500-1

Ma G, Rostami A, Wang T, *et al*., 2020. Global and regional seroprevalence estimates for human toxocariasis: A call for action. Adv Parasitol 109:275-290. https://doi.org/10.1016/bs.apar.2020.01.011

Miller AF, 2012. Superoxide dismutases: ancient enzymes and new insights. FEBS Lett: 586(5):585-595. https://doi.org/10.1016/j.febslet.2011.10.048

Mittra B, Laranjeira-Silva MF, Miguel DC, *et al*., 2017. The iron-dependent mitochondrial superoxide dismutase SODA promotes *Leishmania* virulence. J Biol Chem 292:12324-12338. https://doi.org/10.1074/jbc.M116.772624.

Motavallihaghi S, Khodadadi I, Goudarzi F, *et al*., 2022. The role of *Acanthamoeba castellanii* (T4 genotype) antioxidant enzymes in parasite survival under H_2O_2-induced oxidative stress. Parasitol Int 87:102523.https://doi.org/10.1016/j.parint.2021.102523.

Moustafa A, Perbandt M, Liebau E, *et al*., 2022. Crystal structure of an extracellular superoxide dismutase from *Onchocerca volvulus* and implications for parasite-specific drug development. Acta Crystallogr F Struct Biol Commun 78:232-240. https://doi.org/10.1107/S2053230X22005350.

Oka S, Hirai J, Yasukawa T, *et al*., 2015. A correlation of reactive oxygen species accumulation by depletion of superoxide dismutases with age-dependent impairment in the nervous system and muscles of *Drosophila* adults. Biogerontology 16:485-501. https://doi.org/10.1007/s10522-015-9570-3.

Pfarr K, Heider U and Hoerauf A, 2006. RNAi-mediated silencing of actin expression in adult *Litomosoides sigmodontis* is specific, persistent and results in a phenotype. Int J Parasitol 36:661-669. https://doi.org/10.1016/j.ijpara.2006.01.010.

Pratt AJ, DiDonato M, Shin DS, *et al*., 2015. Structural, Functional, and Immunogenic Insights on Cu,Zn Superoxide Dismutase Pathogenic Virulence Factors from *Neisseria meningitidis* and *Brucella abortus.* J Bacteriol 197:3834-3847. https://doi.org/10.1128/JB.00343-15.

Raulf MK, Lepenies B and Strube C, 2021. *Toxocara canis* and *Toxocara cati* Somatic and Excretory-Secretory Antigens Are Recognised by C-Type Lectin Receptors. Pathogens 9(3):321. https://doi.org/10.3390/pathogens10030321.

Roldán WH, Cavero YA, Espinoza YA, *et al*., 2010. Human toxocariasis: a seroepidemiological survey in the Amazonian city of Yurimaguas, Peru. Rev Inst MedTropSao Paulo 52, 37-42. https://doi.org/10.1590/s0036-46652010000100006.

Rostami A, Ma G, Wang T, *et al*., 2019. Human toxocariasis - A look at a neglected disease through an epidemiological 'prism'. Infect Genet Evol 4:104002. https://doi.org/10.1016/j.meegid.2019.104002.

Rostami A, Riahi SM, Hofmann A, *et al*., 2020. Global prevalence of *Toxocara* infection in dogs. Adv Parasitol 109:561-583. https://doi.org/10.1016/bs.apar.2020.01.017

Schatzman SS and Culotta VC, 2018. Chemical Warfare at the Microorganismal Level: A Closer Look at the Superoxide Dismutase Enzymes of Pathogens. ACS Infect Dis 8:893-903. https://doi.org/10.1021/acsinfecdis.8b00026.

Shalaby KA, Yin L, Thakur A, *et al*., 2003. Protection against *Schistosoma mansoni* utilizing DNA vaccination with genes encoding Cu/Zn cytosolic superoxide dismutase, signal peptide-containing superoxide dismutase and glutathione peroxidase enzymes. Vaccine 22:130-136. https://doi.org/10.1016/s0264-410x(03)00535-8.

Sim C and Denlinger DL, 2011. Catalase and superoxide dismutase-2 enhance survival and protect ovaries during overwintering diapause in the mosquito *Culex pipiens*. J Insect Physiol 57(5):628-634. https://doi.org/10.1016/j.jinsphys.2011.01.012.

Strube C, Heuer L and Janecek E, 2013. *Toxocara* spp. infections in paratenic hosts. Vet Parasitol 193:375-389. https://doi.org/10.1016/j.vetpar.2012.12.033 .

Taghipour A, Habibpour H, Mirzapour A, *et al*., 2021. *Toxocara* infection/exposure and the risk of schizophrenia: a systematic review and meta-analysis. Trans R Soc Trop Med Hyg 115(10):1114-1121.https://doi.org/10.1093/trstmh/trab056.

Vaca-Paniagua F, Torres-Rivera A, Parra-Unda R, *et al*., 2008. *Taenia solium*: antioxidant metabolism enzymes as targets for cestocidal drugs and vaccines. Curr Top Med Chem 8:393-399. https://doi.org/10.2174/156802608783790857.

Wu TL, Wang BN, Yang AJ, *et al*., 2024. C-type lectin 4 of *Toxocaracanis*activates NF-κB and MAPK pathways by modulating NOD1/2 and RIP2 in murine macrophages in vitro. Parasitol Res 123:189.https://doi.org/10.1007/s00436-024-08212-2.

Yang J and Zhang Y, 2015. I-TASSER server: new development for protein structure and function predictions. Nucleic Acids Res 43:W174-W181. https://doi.org/10.1093/nar/gkv342.

Yang Y, Chen Y, Zheng Z, *et al*., 2024. Alterations of plasma circulating microRNAs in BALB/c mice with *Toxocara canis* visceral and cerebral larva migrans. Parasit Vectors 17(1):256. https://doi.org/10.1186/s13071-024-06327-0

Yuan D, Luo S, Xu L, *et al*., 2019. Regulatory effect of host miR-101b-3p on parasitism of nematode *Angiostrongylus cantonensis* via superoxide dismutase 3. Biochem Biophys Acta Gene Regul Mech 1862:557-566.https://doi.org/10.1016/j.bbagrm.2019.02.004.

Zhou RQ, Ma GX, Korhonen PK, *et al*., 2017. Comparative transcriptomic analyses of male and female adult *Toxocara canis*. Gene 600:85-89. https://doi.org/10.1016/j.gene.2016.11.024.

Zhou R, Jia H, Du Z, *et al*., 2022. The non-glycosylated protein of *Toxocara canis* MUC-1 interacts with proteins of murine macrophages. PLoS Negl Trop Dis 16:e0010734. https://doi.org/10.1371/journal.pntd.0010734.

Zhang C, Freddolino L and Zhang Y, 2017. COFACTOR: improved protein function prediction by combining structure, sequence and protein-protein interaction information. Nucleic Acids Res 45:W291-W299. https://doi.org/10.1093/nar/gkx366.

Zheng WB, Zou Y, Zhu XQ, *et al*., 2020. *Toxocara* "omics" and the promises it holds for medicine and veterinary medicine. Adv Parasitol 109:89-108. https://doi.org/10.1016/bs.apar.2020.01.002

Zheng W, Zhang C, Li Y, *et al*., 2021. Folding non-homologous proteins by coupling deep-learning contact maps with I-TASSER assembly simulations. Cell Rep Methods 26:100014. https://doi.org/10.1016/j.crmeth.2021.100014.

Zheng WB, Zou Y, He JJ, *et al*., 2021. Global profiling of lncRNAs-miRNAs-mRNAs reveals differential expression of coding genes and non-coding RNAs in the lungs of beagle dogs at different stages of *Toxocara canis* infection. Int J Parasitol 51:49-61. https://doi.org/10.1016/j.ijpara.2020.07.014.

Zhu XQ, Korhonen PK, Cai H, *et al*., 2015. Genetic blueprint of the zoonotic pathogen *Toxocaracanis*. Nat Commun 6:6145. https://doi.org/10.1038/ncomms7145.

Zimmerman SM and Kim SK, 2014.The GATA transcription factor/MTA-1 homolog egr-1 promotes longevity and stress resistance in *Caenorhabditis elegans*. Aging Cell 13(2):329-339. https://doi.org/10.1111/acel.12179.